# Structurally Related $Me_3M$ Propellers (M = Sn, Pb) in the Solid State: A Comparison Based on Variable-Temperature CP/MAS NMR Results

Jörg Kümmerlen, Angelika Sebald,* and Elke Sendermann

*Bayerisches Geoinstitut, Universität Bayreuth, D-95440 Bayreuth, Germany*

*Received October 19, 1993*®

Jump rates and activation energies of $Me_3M$ (M = Sn, Pb) propeller-like reorientation in the solid state are obtained from one- and two-dimensional variable-temperature $^{13}C$ CP/MAS NMR for two pairs of homologous $Me_3Sn$ and $Me_3Pb$ compounds. The isostructural pair $Me_3Sn(O_2CMe)$, **1**, and $Me_3Pb(O_2CMe)$, **2**, which both form polymeric zigzag chains in the solid state with M in trigonal-bipyramidal $Me_3MO_2$ coordination, display very similar, fairly high activation energies for the $Me_3M$ $2\pi/3$ jump process (**1**, $E_a = 68.5 \pm 6.1$ kJ mol$^{-1}$; **2**, $E_a = 62.1 \pm 6.9$ kJ mol$^{-1}$). This can be rationalized on the basis of comparable intra- and interchain van der Waals interactions in solid **1** and **2**. In contrast to the results for **1** and **2**, the pair of compounds $Me_3M-C\equiv C-MMe_3$ (**3**; M = Sn; **4**, M = Pb), with M in tetrahedral coordination and of unknown single crystal X-ray structure, shows considerably different $Me_3M$ $2\pi/3$ jump rates $\kappa$ at room temperature (**3**, $\kappa = 200$ Hz; **4**, $\kappa = 0.3$ Hz; $T = 298$ K). This latter finding would suggest that this chemically homologous pair, **3** and **4**, may not be isostructural in the solid state.

## Introduction

$2\pi/3$ propeller-like jump reorientation is a common dynamic process for solid trimethyltin compounds.[1-6] For a series of structurally closely related solid compounds $Me_3SnX$–mostly with oxygen-bearing ligands X, leading to polymeric zigzag chains with trigonal-bipyramidal chain-building units $Me_3SnO_2$—we find a very wide range of $2\pi/3$ $Me_3Sn$ jump rates of approximately $10^{-1}$–$10^4$ Hz at ambient temperature, corresponding to activation energies $E_a \approx 20$–$70$ kJ mol$^{-1}$ for this thermally activated process.[1-4] Kinetic data for this dynamic solid-state property of the $Me_3Sn$ moiety can be obtained conveniently from a variety of variable-temperature high-resolution solid-state NMR techniques. Depending on the respective jump rates, one-dimensional $^{13}C$ CP/MAS plus line shape analysis in the exchange broadened regime, two-dimensional $^{13}C$ CP/MAS exchange spectroscopy,[1,2] or $^1H$–$B_1$ irradiation-field dependent $T_2$ processes on the observed $^{13}C$ magnetization[3,4] yield the desired kinetic information, i.e. jump rates as a function of temperature. From these rates the corresponding activation energies are obtained from Arrhenius plots. If we consider these Arrhenius-equation-derived values for $E_a$ as characteristic for the dynamic process, we find that in all cases where the single crystal structure of the respective $Me_3Sn$ compound is known that these activation energies are in close harmony with structural features as determined by X-ray diffraction. This holds true for both *intra-* and *inter*chain van der Waals interactions, defining energy barriers for the jump reorientation. Force field calculations based on geometric information from single crystal X-ray diffraction serve to further corroborate such structure–dynamics correlations.[2]

All experimental evidence concerning $Me_3Sn$ propellers in the solid state, gathered so far from NMR, X-ray diffraction, and force field calculations, raises further questions with respect to cause and effect in the interplay of crystal and molecular structure/order and dynamic processes. One such question which comes to mind is whether the bulk of M in $Me_3M$ propellers in otherwise isostructural compounds will have a strong influence on the dynamic properties of $Me_3M$. Organotin and organolead chemistry offers the opportunity for pairwise comparison of $Me_3Sn$ vs $Me_3Pb$ propellers in the solid state. In this contribution we report NMR results on the dynamic properties of the isostructural pair of compounds $Me_3Sn(O_2CMe)$,[1] **1**, and $Me_3Pb(O_2CMe)$, **2**. While **1** and **2** allow comparison of $Me_3M$ propellers in trigonal-bipyramidal $Me_3MO_2$ coordination, $Me_3M$ propellers in tetrahedral coordination are considered for the two homologous compounds $Me_3Sn-C\equiv C-SnMe_3$, **3**, and $Me_3Pb-C\equiv C-PbMe_3$, **4**.

## Experimental Section

Compounds **1**,[7] **3**,[8] and **4**[8] were synthesized following published procedures; **2** is commercially available (Alfa Products). **3** and **4** are easily hydrolyzed and, therefore, have to be handled under inert gas and were packed in airtight Kel-F inserts[9] for all CP/MAS experiments.

All $^{13}C$, $^{119}Sn$, and $^{207}Pb$ CP/MAS experiments were carried out using a Bruker MSL 300 NMR spectrometer, equipped with the necessary CP/MAS double bearing probes and a Bruker B-VT 1000 temperature control unit. $ZrO_2$ rotors (7-mm-o.d.) with BN end-caps were used for variable-temperature CP/MAS experiments. For **1** and **2** the rotor was completely filled; for **3**

* Abstract published in *Advance ACS Abstracts*, January 15, 1994.

(1) Kümmerlen, J.; Sebald, A. *J. Am. Chem. Soc.* **1993**, *115*, 1134.
(2) Kümmerlen, J.; Lange, I.; Milius, W.; Sebald, A.; Blaschette, A. *Organometallics* **1993**, *12*, 3541.
(3) Kümmerlen, J.; Sebald, A. *Magn. Reson. Chem.*, in press.
(4) Kümmerlen, J.; Sebald, A. *Solid State NMR*, submitted for publication.
(5) Apperley, D. C.; Davies, N. A.; Harris, R. K.; Eller, S.; Schwarz, P.; Fischer, R. D. *J. Chem. Soc., Chem. Commun.* **1992**, 740.
(6) Behrens, U.; Brimah, A. K.; Soliman, T. M.; Fischer, R. D.; Apperley, D. C.; Davies, N. A.; Harris, R. K. *Organometallics* **1992**, *11*, 1718.
(7) Dannley, R. L.; Aue, W. A. *J. Org. Chem.* **1965**, *30*, 3845.
(8) Wrackmeyer, B. *J. Magn. Reson.* **1981**, *42*, 287.
(9) Merwin, L. H.; Sebald, A.; Espidel, J. E.; Harris, R. K. *J. Magn. Reson.* **1989**, *84*, 367.

0276-7333/94/2313-0802$04.50/0 

**Table 1. $^{13}C$, $^{119}Sn$, and $^{207}Pb$ NMR Data for Compounds 1–4 in the Solid State**

| compd | temp (K) | $\delta$ ($^{119}Sn$)/$\delta$($^{207}Pb$) (ppm) | $\delta$ ($^{13}C$) ($Me_3M$)[a] (ppm) | further $\delta(^{13}C)$[a] (ppm) |
|---|---|---|---|---|
| 1, $Me_3Sn(O_2CMe)$[b] | 297 | −27.2 | 1.3; −0.5 (relat intens 2:1) | 25.3; 178.6 |
| 2, $Me_3Pb(O_2CMe)$ | 297 | +211.0 | 18.3; 15.7 (relat intens 2:1) | 25.7; 177.8 |
| 3, $Me_3Sn—C\equiv C—SnMe_3$[c] | 297 | −86.0 | −5.4 [360] | 117.5 [397] |
| | 230 | −85.9 | −4.8 [402]; −5.6 [383]; −5.9 [375] | 117.8 [381] |
| 4, $Me_3Pb—C\equiv C—PbMe_3$[d] | 297 | −168.9 | 6.3 [397]; 4.5 [346]; 1.9 [285] | 116.9 [152; 71] |

[a] Scalar coupling constants $^{1,2}J(M^{13}C)$ (Hz) are given in square brackets; M = $^{119}Sn$, $^{207}Pb$. [b] Data taken from ref 1. [c] From ref 8, data in $C_6D_6$: $\delta(^{119}Sn)$ = −80.9; $\delta(^{13}C)$ (Me) = 8.0 [401], $\delta(^{13}C)$ (≡C) = 115.5 [406; 48]. [d] From ref 8, data in solution: $\delta(^{207}Pb)$ ($CDCl_3$) = −145.6; (in $C_6D_6$) $\delta(^{207}Pb)$ = −158.8; $\delta(^{13}C)$ (Me) = 1.0 [362], $\delta(^{13}C)$ (≡C) = 118.8 [165; 40].

**Table 2. $^{119}Sn$ and $^{207}Pb$ Shielding Tensor Components for 3 and 4[a]**

| compd | $\sigma_{iso}$ (M) (ppm) (M = Sn, Pb) | ppm $\sigma_{11}$ | $\sigma_{22}$ | $\sigma_{33}$ | $\eta$ |
|---|---|---|---|---|---|
| 3, $Me_3Sn—C\equiv C—SnMe_3$ | +86.0 | +172 | +133 | −48 | 0.3 |
| 4, $Me_3Pb—C\equiv C—PbMe_3$ | +168.9 | +473 | +473 | −440 | 0.0 |

[a] Haeberlen's notation[14] is used: $\sigma_{iso} = -\delta_{iso}$; $|\sigma_{33} - \sigma_{iso}| \geq |\sigma_{11} - \sigma_{iso}| \geq |\sigma_{22} - \sigma_{iso}|$. Asymmetry parameter $\eta = (\sigma_{22} - \sigma_{11})(\sigma_{33} - \sigma_{iso})^{-1}$.

and 4 the filled Kel-F insert was contained inside the rotor (reducing the amount of sample to approximately 100 mg). The matching condition for Hartmann–Hahn cross-polarization ($^1H$ 90° pulse length: 5 μs) was set on adamantane ($^{13}C$), $(C_6H_{11})_4Sn$ ($^{119}Sn$), and (*p*-tolyl)$_4Pb$ ($^{207}Pb$), respectively. Isotropic chemical shifts are given with respect to external $Me_4Si$ ($^{13}C$), $Me_4Sn$ ($^{119}Sn$), and $Me_4Pb$ ($^{207}Pb$) as 0 ppm reference. Homebuilt equipment served to control the long-term stability of the MAS frequencies used. Calibration of the variable-temperature unit was achieved by observation of well-documented phase transitions in ultrapure *n*-alkanes $C_{21}H_{44}$ (305.6 K) and $C_{29}H_{60}$ (330.9 K), samarium acetate was used for low-temperature calibration. For 1–4 thermal equilibration and a stable sample temperature under MAS conditions are typically reached after 20–30 min, whereby the line shapes of $^{13}C$ resonances of 1–4 themselves serve as a highly sensitive measure of the stability of the sample temperature.

One- and two-dimensional $^{13}C$ CP/MAS experimental techniques for the determination of jump rates are described in ref 1, together with kinetic data and the activation energy for compound 1. Typical experimental parameters of variable-temperature 1D and 2D $^{13}C$ CP/MAS experiments ($\nu_{rot} \approx 3.5$ kHz) on 2–4 were as follows.

2, $Me_3Pb(O_2CMe)$: 10 2D $^{13}C$ exchange experiments in the temperature range $T$ = 297–350 K, mixing times $\tau_m$ = 10–250 ms, recycle delay 7 s, contact time 3 ms, 24 transients per trace, TD1 = 128 W, TD2 = 256 W.

3, $Me_3Sn—C\equiv C—SnMe_3$: 15 $^{13}C$ CP/MAS experiments (see also Figure 4) in the temperature range $T$ = 190–296 K, recycle delay 5 s, contact time 2 ms, 80–360 transients per experiment.

4, $Me_3Pb—C\equiv C—PbMe_3$: 1 2D $^{13}C$ exchange experiment at $T$ = 298 K, mixing time 600 ms, recycle delay 10 s, contact time 5 ms, 96 transients per trace, TD1 = 96W, TD2 = 256W.

$^{119}Sn$ and $^{207}Pb$ shielding tensor components for 3 and 4, respectively, were obtained by iterative simulation, of the intensity distribution of the spinning sideband patterns in the $^{119}Sn$ and $^{207}Pb$ CP/MAS spectra of 3 and 4 at various different spinning frequencies. Our iterative simulation routine is based on the second moment analysis by Maricq and Waugh.[10] Details concerning our force field calculations (using a commercially available software package, Moby V.1.4[11]) are given in ref 2.

## Results and Discussion

The solid-state NMR parameters of 1–4 are summarized in Table 1, and Table 2 lists the $^{119}Sn$ and $^{207}Pb$ shielding tensor components of 3 and 4. Figures 1–5 illustrate the dynamic NMR properties of solid 1–4.

**(i) $Me_3Sn(O_2CMe)$ (1) and $Me_3Pb(O_2CMe)$ (2).** $Me_3Sn(O_2CMe)$, 1,[12] and $Me_3Pb(O_2CMe)$, 2,[13] are isostructural in the crystalline state, as can be seen from the single crystal X-ray structures of these two compounds.[12,13] In both cases bidentate acetate anions connect trigonal-bipyramidal $Me_3MO_2$ units (M = Sn (1), M = Pb (2)), leading to polymeric zigzag chains. In both cases two of the $Me_3MO_2$ methyl groups are crystallographically equivalent. Taking the greater covalent radius of Pb as compared with Sn into account, no significant differences of bond lengths and bond angles in 1 and 2 occur:[12,13]

| | | | |
|---|---|---|---|
| Pb–O (pm) | 232.7(2) | Sn–O (pm) | 220.5(3) |
| | 255.5(2) | | 239.1(4) |
| Pb–C (pm) | 217.1(3) | Sn–C (pm) | 213.0(4) |
| | 220.2(3) | | 212.7(5) |
| ∠O–Pb–O (deg) | 169.7(8) | ∠O–Sn–O (deg) | 171.6(1) |
| ∠O–Pb–C (deg) | 90.2(9) | ∠O–Sn–C (deg) | 89.5(1) |
| | 83.3(1) | | 83.7(2) |

The $^{13}C$ CP/MAS spectra of $Me_3Sn(O_2CMe)$, 1, do not change as a function of temparature in the temperature range $T$ = 243–333 K. While on the time scale of one-dimensional $^{13}C$ CP/MAS the $Me_3SnO_2$ unit in 1 appears rigid, $^{13}C$ 2D exchange spectroscopy of 1 reveals the presence of slow mutual Me group exchange:[1] The $2\pi/3$ jump rate for solid 1 is low at room temperature (circa 3 Hz), and a series of $^{13}C$ 2D exchange experiments at various temperatures and with different mixing times yields an activation energy $E_a$ = 68.5 ± 6.1 kJ mol$^{-1}$ for the $2\pi/3$ reorientation of the $Me_3SnO_2$ unit in solid 1. Force field calculations[2] on 1, based on the geometrical parameters from single crystal diffraction, reproduce the expected potential energy profile for $2\pi/3$ jump reorientation of the $Me_3SnO_2$ unit. Figure 1a shows this potential energy profile for solid 1 as a function of displacement of the $Me_3SnO_2$ methyl groups from their crystallographic equilibrium position ($\theta$ = 0°). Rotation around the O–Sn–O axis by $\theta$ = 60° leads to a maximum in the potential energy; rotation by another 60° step to $\theta$ = 120° (i.e. to automatically match crystallographic equilibrium again, caused by the symmetry of the $2\pi/3$ propeller) leads to a minimum in potential energy. This profile is maintained over the full 360° rotation around the O–Sn–O axis. This picture of potential energy of the $Me_3SnO_2$ propeller qualitatively supports the proposed $2\pi/3$ jump reorientation mechanism. In terms of actual barrier heights quite some discrepancy between experimentally determined ($E_a$ = 68.5 ± 6.1 kJ mol$^{-1}$) and calculated (barrier height: 125 kJ mol$^{-1}$) data is found (see Figure 1a). This lack of quantitative agreement is easily explained if we consider the limitations of these van der Waals approximation calculations. Within the constraints of an assumed noncooperative, rigid crystal

(10) Maricq, M. M.; Waugh, J. S. *J. Chem. Phys.* **1979**, *70*, 3300.
(11) Springer New Media, Springer Verlag: Berlin, Heidelberg, New York, Tokyo, 1991.
(12) Chih, H.; Penfold, B. R. *J. Cryst. Mol. Struct.* **1973**, *3*, 285.
(13) Sheldrick, G. M.; Taylor, R. *Acta Crystallogr., Sect. B* **1975**, *B31*, 2740.

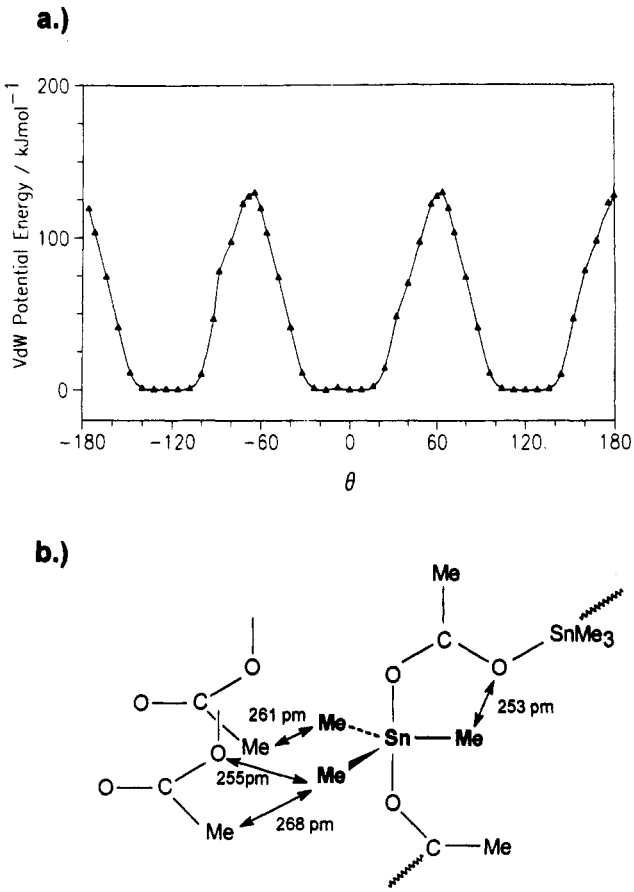


**Figure 1.** Results of force field calculations on solid 1, based on geometric information from the single crystal X-ray structure of 1:[12] (a) relative potential energy profile for the $Me_3SnO_2$ unit as a function of rotation around the O–Sn–O axis ($\theta = 0°$ corresponds to crystallographic equilibrium); (b) schematic representation of the vdW oppressions at the "transition state" of highest potential energy.

lattice, the calculated potential energy barrier heights can only represent the upper possible limit of the respective activation energy, but cannot be directly related to the comparatively slow reorientation/high activation energy in solid 1 as compared with other related $Me_3SnO_2$ propellers.[1-3] Direct comparison of experimental and calculated barrier heights would require force field calculations in a cooperative crystal environment. However, knowing from the results of these force field calculations that a displacement of $\theta = 60°$ from crystallographic equilibrium corresponds to a state of maximum potential energy, we can now further inspect the geometrical constraints and van der Waals oppressions occurring for this particular conformation. This "transition state" of highest potential energy is illustrated in Figure 1b where relevant shortest transition state distances to neighboring groups and oxygen atoms (both *inter*- and *intra*chain) are given. The shortest methyl–oxygen distances of 253 and 255 pm are of intra- and interchain origin, respectively. Both distances are considerably shorter than the sum of vdW radii for a methyl group and an oxygen atom ($r_{vdW}$ = 360 pm). Furthermore, very short methyl–methyl interchain distances of 268 and 261 pm are found for the transition state, both of which are much shorter than the sum of vdW radii for two methyl groups ($r_{vdW}$ = 400 pm). Both these short distances occur between methyl groups of the $Me_3Sn$ propeller and rigid acetate methyl groups in neighboring chains. Such a multitude of vdW oppressions for the transition state of the propeller jump corroborates the fairly high activation energy $E_a = 68.5 \pm 6.1$ kJ mol$^{-1}$ for 1 in comparison with structurally related $Me_3SnO_2$ propellers.[1-4] Based on these transition state considerations, it also seems reasonable to ascribe the origin of the fairly high activation barrier in 1 mainly to interchain interactions.

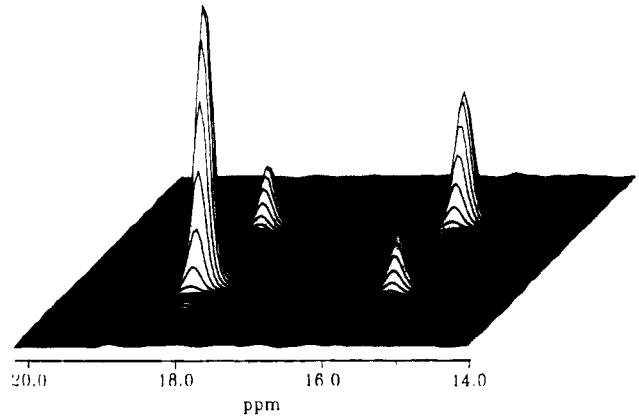


**Figure 2.** $^{13}C$ 2D exchange experiment on $Me_3Pb(O_2CMe)$, 2. Only the methyl region is shown. Parameters: $T$ = 330 K, $\nu_{rot}$ = 3.3 kHz, mixing time $\tau_m$ = 100 ms, 32 transients, TD1 = 128 W, TD2 = 512 W, zero-filled to 512 W in the $\omega_1$-dimension before processing, no symmetrization.

An almost identical picture for $Me_3Pb(O_2CMe)$, 2, emerges from variable temperature 1D and 2D $^{13}C$ and $^{207}Pb$ CP/MAS experiments. The $^{207}Pb$ CP/MAS spectrum of 2 at room temperature ($\delta(^{207}Pb)$ = 211 ppm) shows an almost axially symmetric $^{207}Pb$ shielding tensor with a spinning sideband pattern covering a range of approximately 1600 ppm. As in the case of 1, solid 2 appears rigid on the time scale of 1D $^{13}C$ CP/MAS: in the temperature range $T$ = 298–360 K the $^{13}C$ CP/MAS spectra of 2 are independent of temperature. For this temperature range four $^{13}C$ resonances (acetate, 177.8 and 25.7 ppm; $Me_3Pb$, 18.3 and 15.7 ppm; 2:1 relative intensity) are observed for solid 2. Again, $^{13}C$ 2D exchange spectroscopy reveals the presence of slow mutual methyl group exchange within the $Me_3PbO_2$ moiety in 2 (see Figure 2). From a series of $^{13}C$ 2D exchange spectra we determine the $2\pi/3$ jump rate of 2 as a function of temperature and thus obtain a value of the corresponding activation energy $E_a = 62.1 \pm 6.9$ kJ mol$^{-1}$ for solid 2.

Within experimental error, the NMR-derived activation energies for $2\pi/3$ reorientation of the $Me_3MO_2$ unit in solid 1 and 2 are identical. This NMR finding concerning the dynamic solid-state properties of 1 and 2 is also mirrored by the static picture of 1 and 2 (isostructural) as obtained from single crystal X-ray diffraction. At first glance, it may seem surprising that two different experimental methods with vastly different operative time scales should yield such similar findings of identity for solid 1 and 2. If, however, we consider that both methods ultimately monitor bonding properties in a rather indirect fashion, it seems much more plausible that different $Me_3M$ propellers with M = Sn, Pb of comparable structural constraints will display identical dynamic properties in the solid state. Of course, results obtained so far for only one pair of isostructural compounds, 1 and 2, do not warrant any generalization; more experimental NMR data for isostructural compounds, like 1 and 2, are necessary.

**(ii) $Me_3Sn$—C≡C—$SnMe_3$ (3) and $Me_3Pb$—C≡C—$PbMe_3$ (4).** We consider the molecular unit $Me_3M$—

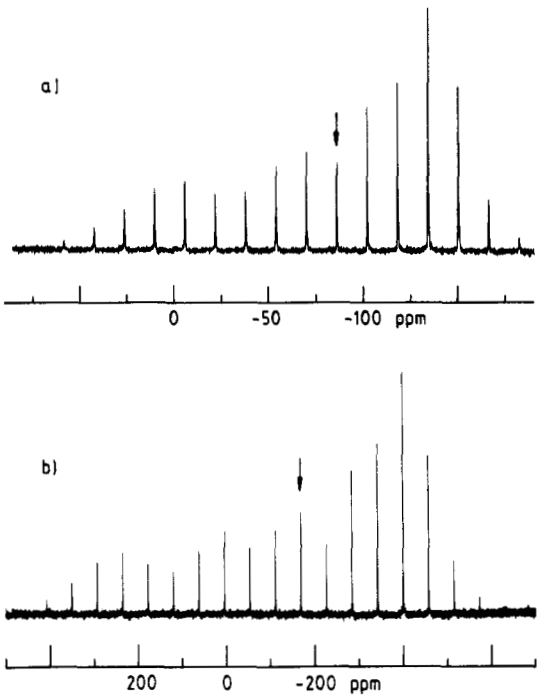


**Figure 3.** $^{119}Sn$ (a) and $^{207}Pb$ (b) CP/MAS spectra of **3** and **4**, respectively, at room temperature. Experimental parameters: (a) $\nu_{rot}$ = 1.8 kHz, contact time 1 ms, recycle delay 4 s, 1588 transients; (b) $\nu_{rot}$ = 3.6 kHz, contact time 5 ms, recycle delay 5 s, 470 transients. Center bands are marked by an arrow.

C≡C—$MMe_3$. The highest possible point group symmetry for this unit is either $D_{3d}$ (staggered conformation) or $D_{3h}$ (eclipsed conformation). If either of these two highest possible symmetries were realized in the solid state for **3** (M = Sn) or **4** (M = Pb), then necessarily the shielding tensor for M would have to be axially symmetric, with its unique component oriented along the M—C≡C—M axis. The single crystal X-ray structures of **3** and **4** are unknown due to a lack of suitable single crystals. We need to further justify our consideration of only *molecular* symmetry for solid **3** and **4**: a comparison of isotropic chemical shifts $\delta(^{119}Sn)$, $\delta(^{207}Pb)$ for **3** and **4** in the solid state and in nonassociating solvents such as $CHCl_3$ and $C_6H_6$[8] shows typical values for tetrahedral $Me_3M$ environments in such compounds; only marginal differences between the solid state-data and data for dilute solutions of **3** and **4**, respectively, are found (see Table 1). Thus, it is justified to consider **3** and **4** also in the solid state as nonassociated molecular units in a first approximation. Within this approximation it will suffice to consider point group symmetry constraints for solid **3** and **4**. In fact, in the absence of single crystal X-ray diffraction information we have no other choice anyway.

The experimental $^{119}Sn$ and $^{207}Pb$ CP/MAS spectra of **3** and **4**, obtained at room temperature, are depicted in Figure 3. In both cases only one sharp resonance is observed for M (M = Sn, Pb), consistent with a molecular structure $Me_3M$—C≡C—$MMe_3$ where both atoms M within a molecule are chemically equivalent. Inspection of the shielding tensor properties of M in **3** and **4** reveals a seemingly striking difference. The $^{207}Pb$ shielding tensor for **4** displays full rotational symmetry (asymmetry parameter $\eta$ = 0.0 in Haeberlen's notation[14]) which, of course, would so far not contradict a $D_{3d}$ or $D_{3h}$ point group symmetry for $Me_3Pb$—C≡C—$PbMe_3$, **4**. In contrast to this finding for solid **4**, the $^{119}Sn$ shielding tensor for **3**,

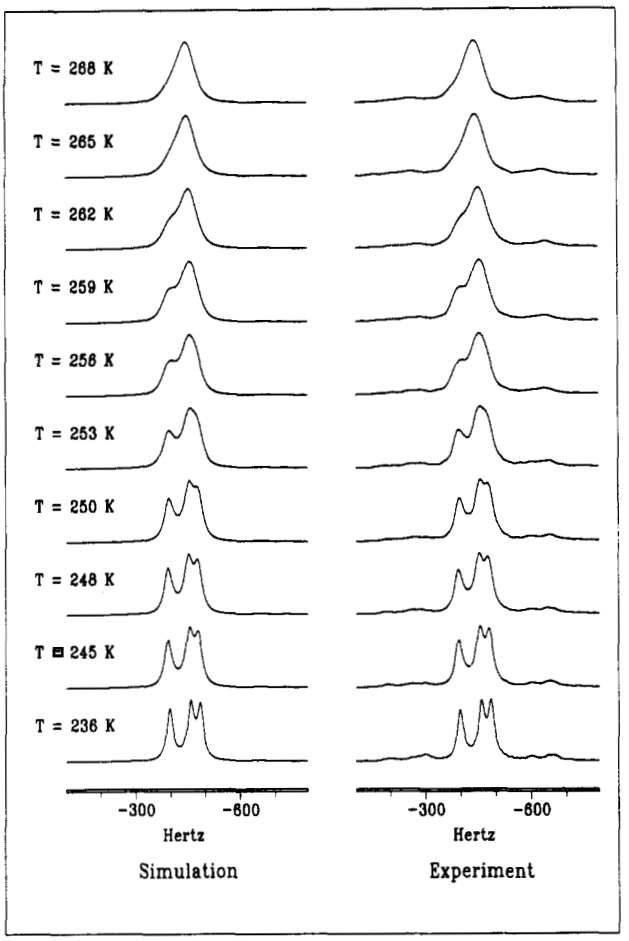


**Figure 4.** Experimental (right) and simulated (left) $^{13}C$ CP/MAS spectra of **3** in the exchange-broadening temperature range $T$ = 236–268 K. Only the methyl region is shown.

$Me_3Sn$—C≡C—$SnMe_3$, does not show full axial symmetry, $\eta$ = 0.3 in this case. A not fully axially symmetric $^{119}Sn$ shielding tensor for **3** is possible if the full $C_3$ rotational symmetry around the Sn—C≡C—Sn axis is lost. Still, also compound **3** must belong to a point group symmetry which leaves the two Sn atoms chemically equivalent.

Further light is shed on these $^{119}Sn$, $^{207}Pb$ shielding tensor considerations by inspection of the $^{13}C$ CP/MAS spectra of **3** and **4**, at which point also $2\pi/3$ reorientation of the tetrahedral $Me_3M$ units in **3** and **4** comes into play. Let us consider a conformationally rigid molecule $Me_3M$—C≡C—$MMe_3$. A molecular symmetry $D_{3d}$ or $D_{3h}$ would render all six methyl groups in such a molecule chemically equivalent. This is, however, not what we observe experimentally. As can be seen from 1D and 2D $^{13}C$ NMR spectra of **3** and **4** (see Figures 4 and 5, respectively), both compounds show—in their respective slow $2\pi/3$ exchange regime—three $^{13}C$ resonances in a 1:1:1 intensity ratio in the methyl region. The $^{13}C$ 2D exchange spectrum of **4** (see Figure 5) proves that mutual exchange between all three resonances occurs, so that necessarily three inequivalent methyl $^{13}C$ resonances must belong to one $Me_3M$ unit. Returning to the static picture of a conformationally rigid molecule $Me_3M$—C≡C—$MMe_3$ we now have further constraints on the possible molecular symmetry of **3** and **4**, as well as possible $^{119}Sn$ and $^{207}Pb$ shielding tensor orientations within the molecular frame

(14) Haeberlen, U. High Resolution NMR in Solids. Selective Averaging. In *Advances in Magnetic Resonance*; Waugh, J. S., Ed.; Academic Press: New York, San Francisco, London, 1976; Supplement 1.

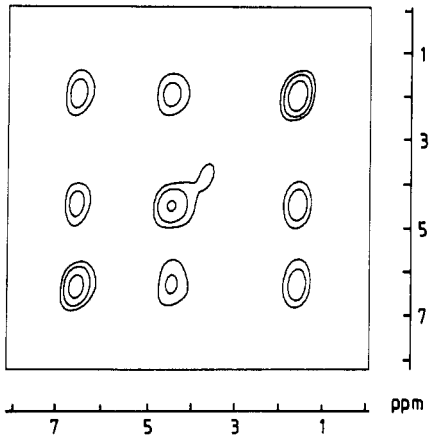


**Figure 5.** $^{13}C$ 2D exchange experiment on **4** at $T$ = 298 K. Only the methyl region is shown. The asymmetric shape of the central $^{13}C$ resonance is not an artifact but due to scalar coupling $^{1}J(^{207}Pb^{13}C)$ of the resonance at 1.9 ppm. $\nu_{rot}$ = 3.5 kHz; further parameters are given in the Experimental Section.

of symmetry of **3** and **4**. Taking the combined $^{13}C$ and $^{119}Sn$, $^{207}Pb$ evidence into account, clearly $C_3$ rotational symmetry around the M—C≡C—M axis is ruled out. The only remaining symmetry operations applicable to the whole $Me_3M$—C≡C—$MMe_3$ molecule in the solid state *and* consistent with all NMR evidence are either a mirror plane ($\sigma$) through the middle of (and perpendicular to) the C≡C bond, corresponding to an eclipsed conformation, or an inversion center (i), corresponding to a staggered conformation of $Me_3M$—C≡C—$MMe_3$. Which of these two possibilities is verified for solid **3** and **4** and, in fact, whether both compounds prefer the same low-temperature conformation or not cannot simply be determined on the basis of powder NMR methods alone. However, the remaining possible symmetry operations $\sigma$ or i for **3** and **4** define further constraints for $^{119}Sn$ and $^{207}Pb$ shielding tensor orientations in **3** and **4**. Clearly, the fact that we observe an axially symmetric $^{207}Pb$ shielding tensor for solid **4** is not strictly required by the remaining possible molecular symmetry of solid **4**, but is an illustrative example that, by chance, the symmetry properties of the shielding tensor of a given nucleus in a molecule can overfulfill the necessary symmetry requirements of the corresponding molecular point group symmetry and may, thus, lead to wrong conclusions concerning molecular symmetry. Given the remaining possible operations, $\sigma$ or i, for solid **4** it is, however, necessary that one of the three $^{207}Pb$ shielding tensor components (two of which are equal, in this case) of **4** be oriented along the Pb—C≡C—Pb axis. Symmetry ($\sigma$ or i) does not dictate which tensor component this should be, but a comparison with data for closely related compounds $R_3M$—C≡C—R′ and $RM(C{\equiv}C{-}R')_3$[15] makes it reasonable to assign the unique, least shielded $^{207}Pb$ shielding tensor component as parallel to the Pb—C≡C—Pb direction for solid **4**. The same arguments hold for the assignment of $^{119}Sn$ shielding tensor components in **3**: of course, molecular symmetry of **3**, restricted to either $\sigma$ or i, is fully in accord with the experimental observation of a nonaxially symmetric $^{119}Sn$ shielding tensor for **3**. Again, the direction of one of the three tensor components is fixed in the molecular frame by either $\sigma$ or i, and by comparison with related compounds[15] it is most likely that, again, this should be the least shielded component.

Before turning our attention to the dynamic solid-state properties of **3** and **4**, a few more general remarks concerning the above symmetry/shielding tensor discussion seem in place. First, the above discussion of compounds **3** and **4** has always implicitly assumed a linear M—C≡C—M arrangement, which seems reasonable from a chemical point of view. From a purely symmetry-related point of view, also deviations from a linear M—C≡C—M arrangement would be possible. Similarly implicitly, to all discussions of MAS or CP/MAS spectra-derived shielding tensor parameters (and asymmetry parameters $\eta$) the modifier "within experimental error" needs to be added. It is well-known[10,16] that the precise determination of shielding tensor components from MAS spectra for cases with axial or nearly axial symmetry tends to be problematic. Obviously, heavy spin $^1/_2$ nuclei such as $^{119}Sn$ or $^{207}Pb$ are particularly suitable candidates to probe molecular symmetry by means of shielding tensor considerations, simply because such nuclei offer exceptional ease of experimentally obtaining shielding tensor components under MAS conditions at the most common external magnetic field strengths $B_0 \approx 4$–7 T. Similar, conformation-related effects on the $^{207}Pb$ shielding tensor components and asymmetry parameter $\eta$ have been reported for centrosymmetric molecules in solid crystalline compounds hexaorganyldilead, $Pb_2R_6$.[17]

Finally, we will consider the $2\pi/3$ $Me_3M$ propeller jump properties of solid **3** and **4**. On the time scale of 1D $^{13}C$ CP/MAS at room temperature, **3**, $Me_3Sn$—C≡C—$SnMe_3$ is in a fast exchange regime, only one—motionally averaged due to $2\pi/3$ reorientation—sharp $^{13}C$ resonance is observed for the $Me_3Sn$ group at −5.4 ppm. This is illustrated in Figure 4 where experimental and simulated variable-temperature $^{13}C$ CP/MAS spectra of **3** are compared. Line shape simulation for the exchange broadened $^{13}C$ regime for **3** yields an activation energy for the $Me_3Sn$ reorientation in **3** of $E_a = 45.8 \pm 2.4$ kJ mol$^{-1}$. The corresponding $2\pi/3$ jump rate at room temperature amounts to approximately $\kappa$ = 200 Hz. It should also be mentioned that this dynamic process is of no consequence for the $^{119}Sn$ shielding tensor in **3**. In order to produce any motional averaging effect on the $^{119}Sn$ shielding tensor in **3**, the $Me_3Sn$ jump rate would have to be at least of the order of magnitude of the width of the static powder pattern of the $^{119}Sn$ resonance in **3**. In our case, that is in the 111.9-MHz $^{119}Sn$ NMR spectrum of **3**, with width of this pattern is approximately 25 kHz.

Inspection of the room-temperature $^{13}C$ 2D exchange spectrum of **4** (see Figure 5) shows immediately that **4**—in contrast to the findings for **3**—is in a slow exchange regime on the time scale of 1D $^{13}C$ NMR at this temperature: three well-resolved sharp $^{13}C$ resonances are observed for the $Me_3Pb$ unit. The relative off-diagonal intensities in the $^{13}C$ 2D exchange experiment on **4** (see Figure 5) correspond to a room-temperature jump rate of $\kappa$ = 0.3 Hz. Of course, the activation energy for the $Me_3Pb$ orientation in solid **4** *should* be determined from a series of 1D or 2D $^{13}C$ CP/MAS experiments. However, solid **4** decomposes at elevated temperatures and further 2D $^{13}C$ exchange experiments on **4** at temperatures below room

(15) Sebald, A.; Sendermann, E. *Magn. Reson. Chem.*, submitted for publication.

(16) Clayden, N. J.; Dobson, C. M.; Lian, L.-Y.; Smith, D. J. *J. Magn. Reson.* **1986**, *69*, 476.

(17) Sebald, A.; Harris, R. K. *Organometallics* **1990**, *9*, 2096.

temperature are severely hampered by massive signal-to-noise problems due to the low exchange rate and the onset of $T_1$ effects. Therefore, it is unfortunately not possible to experimentally determine the activation energy of $2\pi/3$ reorientation in solid **4**: at lower temperatures even very long mixing times $\tau_m$ in $^{13}C$ 2D exchange experiments on **4** only yield off-diagonal resonances of very low relative intensities which cannot be integrated with the necessary precision in order to determine the activation energy for solid **4**.

For the, chemically speaking, homologous pair of compounds **3** and **4** we can only compare the respective $2\pi/3$ jump rates at room temperature, and these are quite different (**3**, $\kappa$ = 200 Hz; **4**, $\kappa$ = 0.3 Hz). In the absence of single crystal X-ray diffraction we cannot answer the question why $2\pi/3$ reorientation in **4** should be so much slower than in **3**. Whether this different dynamic behavior in **3** and **4** is due to intramolecular effects (conformation) or due to intermolecular solid-state effects like packing in the crystal, or both, has to remain a matter of speculation as long as the single crystal structures of **3** and **4** are unknown. In the light of our findings for the isostructural pair of compounds $Me_3M(O_2CMe)$ (**1**, M = Sn; **2**, M = Pb), however, we would predict that **3** and **4** may not be isostructural in the solid state.

**Acknowledgment.** Support of our work by the Deutsche Forschungsgemeinschaft and the Fonds der Chemischen Industrie is gratefully acknowledged. We thank F. Seifert, Bayerisches Geoinstitut, for his continued support and B. Wrackmeyer, Universität Bayreuth, for his generous donation of compounds **3** and **4**.

OM930719Y